NANO LETTERS

pubs.acs.org/NanoLett

Role of Symmetry Breaking on the Optical Transitions in Lead-Salt Quantum Dots

Gero Nootz,*[,†,‡] Lazaro A. Padilha,*[,†] Peter D. Olszak,[†] Scott Webster,[†] David J. Hagan,[†,‡] Eric W. Van Stryland,[†,‡] Larissa Levina,[§] Vlad Sukhovatkin,[§] Lukasz Brzozowski,[§] and Edward H. Sargent[§]

[†]CREOL & FPCE: The College of Optics and Photonics, University of Central Florida, Orlando, Florida 32816, [‡]Physics Department, University of Central Florida, 4000 Central Florida Boulevard, Orlando, Florida 32816, and [§]The Edward S. Rogers Sr. Department of Electrical and Computer Engineering, University of Toronto, Toronto, ON, Canada, M5S3G4

ABSTRACT The influence of quantum confinement on the one- and two-photon absorption spectra (1PA and 2PA) of PbS and PbSe semiconductor quantum dots (QDs) is investigated. The results show 2PA peaks at energies where only 1PA transitions are predicted and 1PA peaks where only 2PA transitions are predicted by the often used isotropic $k \cdot p$ four-band envelope function formalism. The first experimentally identified two-photon absorption peak coincides with the energy of the first one photon allowed transition. This first two-photon peak cannot be explained by band anisotropy, verifying that the inversion symmetry of the wave functions is broken and relaxation of the parity selection rules has to be taken into account to explain optical transitions in lead-salt QDs. Thus, while the band anisotropy of the bulk semiconductor plays a role in the absorption spectra, especially for the more anisotropic PbSe QDs, a complete model of the absorption spectra, for both 1PA and 2PA, must also include symmetry breaking of the quantum confined wave functions. These studies clarify the controversy of the origin of spectral features in lead-salt QDs.

KEYWORDS Quantum-dots, two-photon absorption, inversion symmetry, selection rules, nonlinear spectroscopy

Semiconductor quantum dots (QDs) have been intensively investigated because they are promising candidates for novel devices and allow the study of quantum effects in a relatively simple system. The lead-salt bulk semiconductors, PbS and PbSe, possess unique electronic structure of a narrow band gap together with small and nearly equal effective masses of the carriers in the conduction and valence bands. In QDs, this leads to strong quantum confinement for both carriers, and large tunability of the one-photon absorption (1PA) and two-photon absorption (2PA) spectra with QD size. The quantum confined energy levels in this system can be calculated from a simple isotropic $k \cdot p$ four-band envelope function formalism.[1] In this model, the QDs are treated as ideal spheres in which the constituent atoms are symmetrically distributed around the center of the sphere. Hence the electronic wave functions possess well-defined symmetry and the possible 1PA and 2PA transitions must obey strict but opposite parity selection rules. However, due to the observation of 1PA peaks in the linear absorption spectra at energies where the parity selection rules only allow 2PA transitions, that is, $1S_h \rightarrow 1P_e$ and $1P_h \rightarrow 1S_e$ transitions, the robustness of the parity selection rules, and the validity of the isotropic model in its entirety are currently under intense and controversial discussion.[2−12]

Some authors address the nature of the second observed 1PA peak by considering the band anisotropy of the bulk either in the $k \cdot p$ four-band envelope, formalism[2,3] or in atomistic pseudopotential calculations.[4,5] Because of the band anisotropy, the $1P_{h,e}$ levels are spread in energy, leading to 1PA transitions ($1P_h \rightarrow 1P_e$) that energetically coincide with the 2PA allowed $1S_h \rightarrow 1P_e$ and $1P_h \rightarrow 1S_e$ transitions for PbSe QDs, potentially explaining the extra one-photon transitions not predicted by the isotropic $k \cdot p$ model. However, band anisotropy still fails to predict the second peak in PbS QDs which are more isotropic,[2,3] and moreover does not predict 2PA transitions at the $1S_h \rightarrow 1S_e$ energy for both PbS and PbSe. Other approaches predict that the inversion symmetry of the wave functions is broken in lead-salt QDs allowing optical transitions which are parity forbidden according to the simple $k \cdot p$ four-band envelop function formalism.[6,7] However, to date, there is no consensus in the literature for the physical origin of such symmetry breaking and the resulting transition strength.

Figure 1 shows a schematic of the possible 1PA and 2PA transitions according to the different models. Figure 1a shows the allowed transitions of the isotropic $k \cdot p$ model with strict parity selection rules,[1] Figure 1b shows only parity allowed transitions but takes into account the splitting of the electronic states due to anisotropy, and Figure 1c includes the formally parity forbidden transitions of the isotropic bands that become allowed by breaking the parity selection rules.[6] Note from Figure 1c that only the model considering symmetry breaking predicts two-photon transitions at the

*To whom correspondence should be addressed. E-mail: (G.N.) gnootz@creol.ucf.edu; (L.A.P.) padilha@creol.ucf.edu.

Received for review: 05/26/2010
Published on Web: 08/24/2010

DOI: 10.1021/nl1018673 | *Nano Lett.* **2010,** *10,* 3577–3582

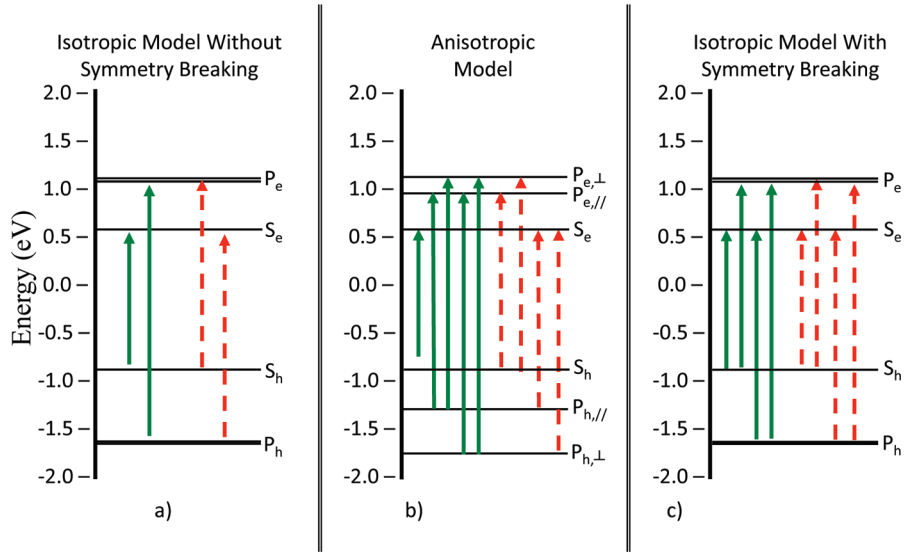

FIGURE 1. Schematic diagram of three different theoretical approaches for the one- and two-photon transitions in lead salt QDs. One-photon transitions are indicated by green/solid lines, two-photon transitions are indicated by red/dashed lines. (a) Parity-allowed transitions according to the isotropic $k \cdot p$ four-band envelope function formulism. (b) Parity-allowed transitions considering the anisotropy of the PbSe bulk semiconductor. (c) Possible one-and two-photon transitions if the principal parity forbidden transitions are allowed.

same energy as the one-photon allowed $1S_h \rightarrow 1S_e$ transition. A possible mechanism leading to the breaking of the selection rules will be discussed later in this paper.

Despite the fact that most studies on this topic have been performed on PbSe QDs,[8−11] we find that PbS QDs are better suited to study the origin of the second peak in the linear absorption spectra. This is because of the more isotropic bands and the nearly identical effective masses of holes and electrons in PbS that lead to an even spacing of the quantum confined levels in the respective bands. So, in this work we perform a comparative study of the 1PA and 2PA spectra of both PbS and PbSe QDs of different sizes. We observe 2PA peaks at the energy of the first 1PA allowed transition ($1S_h \rightarrow 1S_e$) for PbS and PbSe QDs, which cannot be explained by any model that considers only anisotropy,[2−4] verifying that the breaking of the inversion symmetry in lead-salt QDs has to be considered when studying optical transitions. Furthermore, we show experimentally that the breaking of the parity selection rules depends on the QD size and becomes stronger with decreasing radius.

The samples investigated in this work are oleic acid-capped colloidal PbS and PbSe QDs suspended in toluene. The PbS quantum dots were synthesized using an organometallic route previously described in ref 13. Greater detail on the sample synthesis and preparation can be found in the Supporting Information.To calculate the energies and oscillator strengths of the two-photon transitions we use the electronic structure for lead-salt QDs as calculated by the isotropic $k \cdot p$ four-band envelope function formalism developed by Kang and Wise.[1] The wave functions are given in terms of the total angular momentum, j, the z-projection of the angular momentum, m, the total number of zeros of the radial function within the boundaries of the QD, n, and the parity, π. The spherical symmetry of the model predicts states which are energy degenerate in m, and here we only consider transitions involving $n = 1$ since the energies of transitions between initial and final states with $n > 1$ are higher than the transition energies studied by 2PA spectroscopy. Therefore, the individual transitions can be labeled only by j and π according to the initial state in the valence band $|j_v,\pi_v\rangle$ and the final state in the conduction band $|j_c,\pi_c\rangle$. This model results in states with well-defined parity ($\pi = +$ for even parity and $\pi = -$ for odd), leading to strict selection rules for 1PA and 2PA transitions. For simplicity, we adopt the more commonly used nomenclature for the quantum confined state ($1S_{h,e}$, $1P_{h,e}$, $1D_{h,e}$, etc), where S, P, D correspond to $l = 0$, 1, 2, respectively (l is the orbital angular momentum of the dominant term in the mixed wave functions of the quantum confined state).[4] For example, $|1/2, +\rangle \rightarrow |1/2, -\rangle$ is $1S_h \rightarrow 1S_e$, $|1/2, +\rangle \rightarrow |3/2, +\rangle$ is $1S_h \rightarrow 1P_e$, $|3/2, -\rangle \rightarrow |1/2, -\rangle$ is $1P_h \rightarrow 1S_e$ and so on.

In general, the matrix element for a degenerate two-photon transition from a valence band to a conduction band state, $M_{v,c}$ can be calculated as[14−16]

$$M_{v,c} = \sum_i \frac{\langle \Psi_c | e \cdot p | \Psi_i \rangle \langle \Psi_i | ep | \Psi_v \rangle}{E_i - E_v - \hbar\omega} \qquad (1)$$

The sum is over all intermediate states, Ψ_i, which are the one-photon accessible states in the valence or conduction band. Thus a two-photon transition is composed of an intraband and an interband transition and obeys parity selection rules opposite from the 1PA transitions, that is, $\pi_v\pi_i = -1$ for 1PA (for example, $1S_h \rightarrow 1S_e$) and $\pi_v\pi_c = +1$ for 2PA (for example, $1S_h \rightarrow 1P_e$).

DOI: 10.1021/nl1018673 | *Nano Lett.* **2010,** *10,* 3577--3582

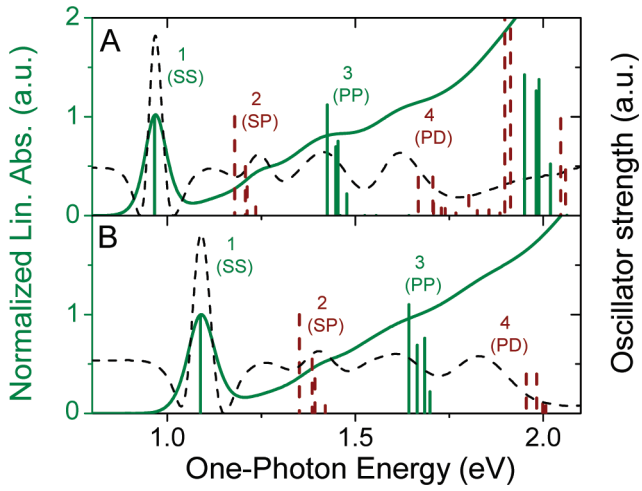

FIGURE 2. Linear absorption spectrum of PbS QDs (solid green lines) and inverted second derivative (dashed black line) indicating identifiable transitions. Calculated one and two photon transitions are shown as vertical lines (green/solid are one photon transitions, red/dashed lines are two photon transitions). Transition 1 (SS) and 3 (PP) occur at energies where one photon transitions are theoretically predicted, but transitions 2 (SP) and 4 (PD) are at energies where the theory only predicts two-photon allowed transitions.

The two-photon transition rate is than calculated from

$$W = \frac{2\pi}{\hbar}\sum_{v,c}|M_{v,c}|^2\delta(E_c - E_v - 2\hbar\omega) \qquad (2)$$

In Figure 2 we compare the 1PA and 2PA transitions predicted by the four-band envelope function model with the linear absorption of two PbS QDs with the $1S_h \rightarrow 1S_e$ peak at 0.97 and 1.09 eV (at room temperature). Because of the nearly equal effective masses of the carriers in the valence and conduction bands,[1] the allowed 1PA and 2PA transitions are grouped together in narrow energy ranges. As previously observed by several authors in PbSe QDs,[8,9] our measurements in PbS QDs, show that the second peak in the linear absorption spectrum occurs at the same energy of the first group of theoretically predicted 2PA transitions (1Sh → 1Pe and 1Ph → 1Se), which are 1PA parity forbidden transitions (see Figures 2 and 3). Because of this good agreement it has been suggested that the second peak in the linear absorption spectrum should be attributed to these parity forbidden transitions that become allowed due to the breaking of the inversion symmetry of the wave functions[8,9] (It should be noted that the two-photon transitions in Figure 2 only indicate the energies at which the theoretically forbidden one-photon transitions occur, but do not reflect their magnitudes). Subsequent experimental observation[15] of a strong 2PA peak with the energy of the nearly degenerate $1S_h \rightarrow 1P_e$ and $1P_h \rightarrow 1S_e$ transitions confirmed the existence of two-photon allowed transitions at these energies in agreement with the predictions by the $k \cdot p$ model. In Figure 2 we show that the fourth identifiable peak in the 1PA spectrum agrees with the second group of 2PA allowed transitions ($1P_h \rightarrow 1D_e$ and $1D_h \rightarrow 1P_e$) at energies where one-photon transitions are not expected (see Figure 2, feature 4). Therefore, in analogy to the second peak in the linear absorption spectra, this fourth feature may also be explained by the breaking of the inversion symmetry.

Comparing the magnitude of the second linear absorption peak in PbS QDs from Figure 2 to the magnitude of the second peak in PbSe QDs from the literature,[17−19] it appears that the peak is less pronounced in PbS. This could be an indication that while the second peak in PbSe QDs is due to contributions from anisotropy and symmetry breaking, the weaker second peak in PbS has its origin in symmetry breaking alone.

With the assumption, justified by the extra peaks in the 1PA spectra, that the parity selection rules are weakened in these QDs, one would expect to observe 2PA at energies corresponding not only to the parity allowed two-photon transitions ($1S_h \rightarrow 1P_e$ and $1P_h \rightarrow 1S_e$) but also to the two-photon forbidden ones ($1S_h \rightarrow 1S_e$ and $1P_h \rightarrow 1P_e$).

To verify this expectation of having 2PA peaks at energies of the 1PA peaks, we have performed 2PA spectroscopy in a series of PbS and PbSe QDs.

The 2PA spectroscopy is performed using an optical parametric generator/amplifier, tunable from 300 nm to 11 μm (TOPAS-800) pumped by 780 nm, 140 fs, 1.2 mJ pulses from a Ti:Sapphire regenerative amplifier (Clark-MXR, model 2010) operating at 1 kHz repetition rate. The samples are investigated at room temperature by either open-aperture Z-scan[20] or two-photon excited fluorescence (2PF).[21] Both techniques measure the 2PA of the QDs. While 2PF is a more rapid technique, it is a relative measurement and needs to be calibrated against a known reference. Furthermore, because of our 2PF detection system we are limited to samples that fluoresce at wavelengths shorter than 800 nm. The Z-scan technique, on the other hand, allows us to obtain a direct absolutely calibrated measurement of the 2PA spectrum. For the Z-scan experiments we use large area Si and Ge photodiodes for wavelengths up to 1.7 μm and Thorlabs PDA30G PbS detectors for longer-wavelength measurements. Further details on the experimental methods and techniques are provided in the Supporting Information.

Figure 3 shows the measured 2PA spectra for different sizes of PbS and PbSe QDs together with their linear absorption and the predicted one- and two-photon transitions. The one- and two-photon transitions energy are calculated relatively to the $1S_h \rightarrow 1S_e$ energy position, that is, for a quantum dot size adjusted to match the energy of the first one-photon transition. Then, the four-band envelope function model works well to provide the relative position of the first allowed 1PA transition and the first 2PA allowed transitions for larger PbS and PbSe. For smaller QDs, due to the overestimated confinement energies, the theory predicts a larger spread between these transitions than experimentally observed.[1]

DOI: 10.1021/nl1018673 | *Nano Lett.* **2010,** *10,* 3577–3582

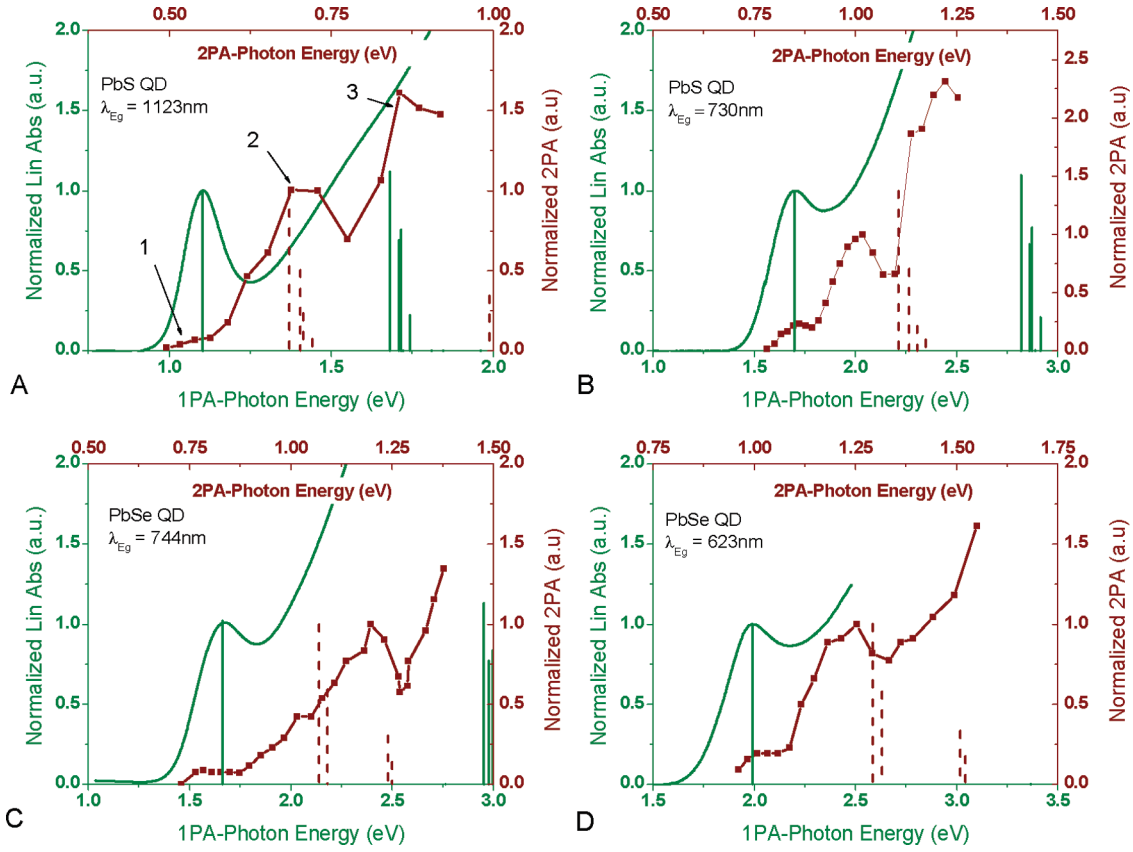

FIGURE 3. One- and two-photon absorption spectra for PbS and PbSe QDs of different sizes together with the theoretically predicted one- and two-photon transitions. The 1PA spectrum is drawn as solid green lines and the 2PA spectra as red lines plus symbols. Theoretical one- and two-photon transitions at their respective energies are vertical lines with their height indicating the oscillator strength (one-photon transitions are green/solid lines, two-photon transitions are red/dashed lines).

For the PbS QDs studied we are able to identify three peaks in the 2PA spectrum. For example, for PbS QDs in Figure 3a the peaks are identified at ~1.10, ~1.35, and ~1.60 eV. For the second PbS QDs in Figure 3 (panel b), the peaks are located at ~1.70, ~2.03, and ~2.44 eV. For the small QDs in Figure 3b,d, the $k \cdot p$ model is known to overestimate the quantum confinement energies.[1] The first predicted 2PA transition is blue shifted by about 0.20 eV from the experimentally observed peak in Figure 3b and about 0.3 eV for the PbSe QD in Figure 3d. These features are observed for a third sample with nearly identical energies as those in Figure 3a (first peak at 1.13 eV, not shown). However, for all samples shown in Figure 3 only the second observed 2PA transition is parity allowed according to the model. The first, and in the case of the PbS samples the third 2PA feature, occur at energies for which the model predicts the first and the second 1PA-allowed transitions ($1S_h \rightarrow 1S_e$ and $1P_h \rightarrow 1P_e$, respectively), as shown by the green lines in Figure 3 (note that, in Figure 3b, as for the second 2PA peak, the third 2PA peak is red shifted compared to the predicted $1P_h \rightarrow 1P_e$ transitions). The third two-photon transition cannot be measured for all samples, since the transitions are close to the 1PA edge, and the size inhomogeneity prevents us from investigating the 2PA spectrum for photon energies larger than ~0.85 × E_g. However, for all samples we observe a strong increase of 2PA at energies higher than the first two-photon allowed peak, suggesting the presence of a close third 2PA peak possibly corresponding to the $1P_h \rightarrow 1P_e$ transitions. For the PbSe QDs, the second group of allowed 2PA transitions is predicted to be at least 1 eV higher in energy than the features measured here. The presence of 2PA peaks at energies corresponding to the $1S_h \rightarrow 1S_e$ and $1P_h \rightarrow 1P_e$ transitions confirms that the inversion symmetry of the wave functions are broken and need to be considered in the analysis of optical transitions and electronic structures of lead-salt quantum dots.

As can be seen in Figure 3, the magnitude of the 2PA at the $1S_h \rightarrow 1S_e$ transition increases with decreasing QD radius for PbS and PbSe. This is evident by comparing the ratio of the magnitude of the 2PA at the energy of the first one-photon allowed transition ($1S_h \rightarrow 1S_e$ transition) and the magnitude of the 2PA at the energy of the allowed $1P_h \rightarrow 1S_e$ and $1S_h \rightarrow 1P_e$ transitions as shown in Figure 4. A similar trend is observed if one compares the ratio between the third and second 2PA peaks measured in PbS QDs (Figure 3). The relative strengthening of the formally parity forbidden 2PA (at $1S_h \rightarrow 1S_e$ and $1P_h \rightarrow 1P_e$) compared to the magnitude of the allowed ($1P_h \rightarrow 1S_e$ and $1S_h \rightarrow 1P_e$) 2PA peaks with

DOI: 10.1021/nl1018673 | *Nano Lett.* **2010,** *10,* 3577–3582

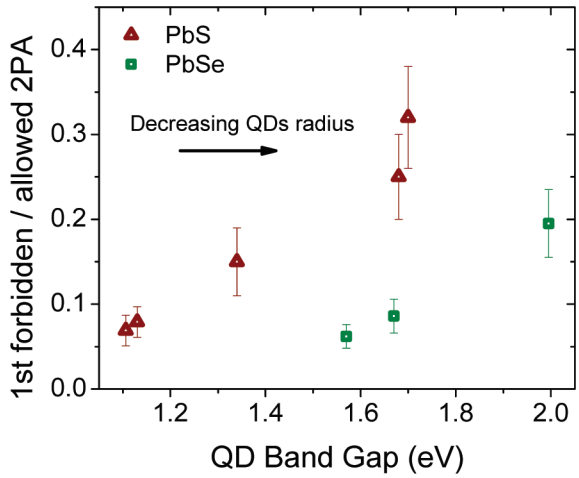

FIGURE 4. Ratio of the 2PA values at the energy of the first one-photon allowed transition divided by the 2PA cross section at the energy of the first group of two-photon allowed transitions plotted versus the band gap of the QDs.

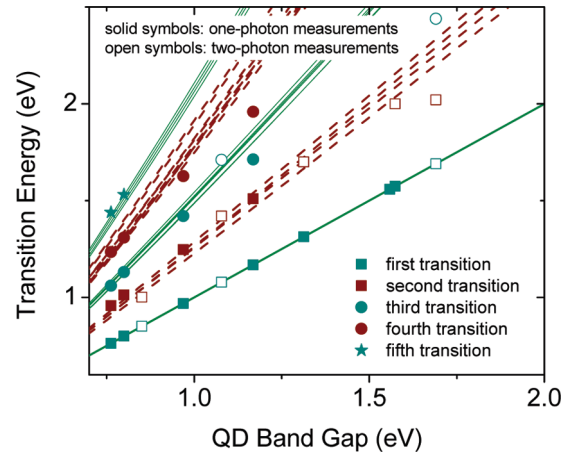

FIGURE 5. Transition energies in PbS QDs as measured by one and two-photon experiments plotted verses the QD band gap (energy of the first absorption peak). Transitions identified in the linear spectrum are shown as solid symbols while the open symbols are measured by either Z-scan or 2PF. Theoretical predictions are shown as green/solid lines and red/dashed lines for parity-conserving transitions and transitions between states of different parity, respectively.

decreasing QD radii indicates that the mechanism responsible for the breaking of the parity selection rules originates from the quantum confinement. As suggested in ref 6, this may be due to the shift of the crystal lattice away from the QD spherical center thereby spoiling the perfect inversion symmetry of the wave functions so that forbidden transitions become allowed. A shift of the center atom away from the center of the QD will have a more pronounced effect for the smallest QDs in this study which, from the estimated sizes, have only ~7 atoms across the diameter, as compared to ~13 atoms across for the largest dots. Furthermore, Bao et al.[7] have theoretically shown that, due to the asymmetric distribution of Pb and Se(S) in the QDs, the wave functions lack inversion symmetry, resulting in strong contribution of the $1P_h \rightarrow 1S_e$ and $1S_h \rightarrow 1P_e$ transitions on the one-photon absorption spectrum, which is amplified in smaller QDs. This is in agreement with our results and is a further indication that the inversion symmetry, which is assumed in the simple $k \cdot p$ approach,[1] is weakened especially for small lead-salt QDs.

The experimental observation of 2PA at the $1S_h \rightarrow 1S_e$ energy for PbSe QDs is in contrast to the results of ref 15 where 2PA at the position of the first 1PA allowed transition was not found. This is despite their observation of relatively strong 1PA at the energy of the first allowed two-photon transition ($1P_h \rightarrow 1S_e$ and $1S_h \rightarrow 1P_e$) in PbSe QDs. Our results show that the 2PA at the $1S_h \rightarrow 1S_e$ energy is appreciable only for small PbSe QDs with a band gap larger than ~1.55 eV, and the samples studied in ref 15 were notably larger than the ones investigated here (the smallest dot studied in ref 15 has a band gap of ~1.05 eV).

While the results from Figures 2, 3, and 5 show that the parity selection rules are broken in both PbS and PbSe QDs, from Figure 4 it is evident that the effect is stronger in PbS QDs. The reason for the smaller parity-forbidden 2PA peak in PbSe QDs is still not completely understood. One possible explanation could be the difference in energy separation of the valence quantum confined energy levels in PbSe and PbS QDs,[1] which would result in smaller intermediate state resonance enhancement for PbSe (denominator in eq 1). However, for the QD sizes investigated here, the intermediate state resonances are very similar for PbS and PbSe QDs and do not account for the difference in the magnitude of the 2PA at the $1S_h \rightarrow 1S_e$ transition energy.

It is important to point out the difference between the relative magnitudes of the parity forbidden transitions in 1PA and 2PA for PbS and PbSe QDs. As mentioned before, comparing the linear absorption spectra of PbS and PbSe QDs (see for example Figure 2 and ref 17 and Figure 1 in refs 18 and 19), it is evident that the second 1PA peak in PbSe QDs is at least comparable, but usually more pronounced, than the one in PbS QDs. However, comparing the 2PA spectrum, one sees that the ratios between the magnitude of the formally parity forbidden and parity allowed 2PA in PbSe is lower than in PbS (Figure 4), indicating a stronger breaking of the inversion symmetry in PbS than in PbSe. So, while the measured 2PA peak at the $1S_h \rightarrow 1S_e$ transition shows that symmetry breaking needs to be considered to fully describe optical transitions in lead-salt QDs, the relatively stronger second peak in the 1PA spectra of PbSe versus PbS suggests that this second peak in PbSe is actually a combination of transitions due to band anisotropy and breaking of the inversion symmetry, with the latter being stronger for smaller QDs and probably negligible for PbSe QDs with band gaps lower than ~1.2 eV. This interpretation is consistent with recent experiments[10,11] that show that for PbSe QDs with band gap from 0.6 − 1.0 eV the second 1PA peak does not include S levels but are mainly contributions of the symmetry allowed $P_{//} \rightarrow P_{//}$ transition due to the band anisotropy.

DOI: 10.1021/nl1018673 | Nano Lett. 2010, 10, 3577–3582

Figure 5 summarizes the identifiable features in the one- and two-photon spectra of PbS QDs and shows good agreement with the isotropic $k \cdot p$ four-band envelope function formalism[1] up to the fifth transition and over a wide range of QD sizes. This illustrates that, for the more isotropic PbS QDs, all measurable features are predicted by the model if formally parity forbidden transitions are included.

In conclusion, we have performed a comparative study of the 2PA spectra of PbS and PbSe QDs using a simple $k \cdot p$ four-band envelope model to gain a qualitative understanding of the observed physical properties. We show that, as is the case for the one-photon transitions where features are observed at energies for which only two-photon transitions are predicted ($1P_h \rightarrow 1S_e$ and $1S_h \rightarrow 1P_e$), 2PA peaks are observed at energies where only one-photon transitions are expected ($1S_h \rightarrow 1S_e$ and $1P_h \rightarrow 1P_e$). Models considering only the anisotropy of the bulk semiconductor do not predict the observed 2PA peak at the $1S_h \rightarrow 1S_e$ transition. So, while we cannot discard the possibility of additional transitions due to band anisotropy to contribute to the 1PA and 2PA spectra, especially for PbSe QDs, the presence of a 2PA peak at the energy of the 1PA, $1S_h \rightarrow 1S_e$, transition proves that breaking of the inversion-symmetry of the wave functions has to be included to fully explain the one- and two-photon spectra of these materials. In addition, the size dependence of the magnitude of the parity forbidden 2PA transitions indicates that the breaking of the inversion symmetry is stronger for smaller QDs, that is, it is due to quantum confinement.

Acknowledgment. This material is based upon work supported in part by the U.S. Army Research Office under Contract/Grant 50372-CH-MUR, the Air Force Office of Sponsored Research MURI AFOSR Grant FA9550-06-1-0337, the DARPA ZOE program Grant W31R4Q-09-1-0012, and the Israel Ministry of Defense contract 993/54250-01 and by Award No. KUS-I1-009-21, made by King Abdullah University of Science and Technology (KAUST). We also would like to thank Frank W. Wise for helpful discussions.

Supporting Information Available. Chemical synthesis and sample preparation and experimental technique. This material is available free of charge via the Internet at http://pubs.acs.org.

REFERENCES AND NOTES

(1) Kang, I.; Wise, F. W. *J. Opt. Soc. Am. B* **1997**, *14*, 1632.
(2) Andreev, A. D.; Lipovskii, A. A. *Phys. Rev. B* **1999**, *59*, 15402.
(3) Tudury, G. E.; Marquezini, M. V.; Ferreira, L. G.; Barbosa, L. C.; Cesar, C. L. *Phys. Rev. B* **2000**, *62*, 7357.
(4) Franceschetti, A.; Luo, J. W.; An, J. M.; Zunger, A. *Phys. Rev. B* **2009**, *79*, 241311(R).
(5) An, J. M.; Franceschetti, A.; Dudiy, S. V.; Zunger, A. *Nano Lett.* **2006**, *6*, 2728.
(6) Goupalov, S. V. *Phys. Rev. B* **2009**, *79*, 233305.
(7) Bao, H.; Habenicht, B. F.; Prezhdo, O. V.; Ruan, X. *Phys. Rev. B* **2009**, *79*, 235306.
(8) Du, H.; Chen, C.; Krishnan, R.; Krauss, T. D.; Harbold, J. M.; Wise, F. W.; Thomas, M. G.; Silcox, J. *Nano Lett.* **2002**, *2*, 1321.
(9) Wehrenberg, B. L.; Wang, C.; Guyot-Sionnest, P. *J. Phys. Chem. B* **2002**, *106*, 10634.
(10) Trinh, M. T.; Houtepen, A. J.; Schins, J. M.; Piris, J.; Siebbeles, L. D. A. *Nano Lett.* **2008**, *8*, 2112.
(11) Liljeroth, P.; Zeijlmans van Emmichoven, P. A.; Hickey, S. G.; Weller, H.; Grandidier, B.; Allan, G.; Vanmaekelbergh, D. *Phys. Rev. Lett.* **2005**, *95*, No. 0868011.
(12) Allan, G.; Delerue, C. *Phys. Rev. B* **2004**, *70*, 245321.
(13) Hines, M. A.; Scholes, G. D. *Adv. Mater.* **2003**, *15*, 1844.
(14) Hutchings, D. C.; Van Stryland, E. W. *J. Opt. Soc. Am. B* **1992**, *9*, 2065.
(15) Peterson, J. J.; Huang, L.; Delerue, C.; Allan, G.; Krauss, T. D. *Nano Lett.* **2007**, *7*, 3827.
(16) Padilha, L. A.; Fu, J.; Hagan, D. J.; Van Stryland, E. W.; Cesar, C. L.; Barbosa, L. C.; Cruz, C. H. B.; Buso, D.; Martucci, A. *Phys. Rev. B* **2007**, *75*, No. 075325.
(17) Schaller, R. D.; Pietryga, J. M.; Goupalov, S. V.; Petruska, M. A.; Ivanov, S. A.; Klimov, V. I. *Phys. Rev. Lett.* **2005**, *95*, 196401.
(18) Moreels, I.; Lambert, K.; Smeets, D.; Muynck, D. D.; Nollet, T.; Martins, J. C.; Vanhaecke, F.; Vantomme, A.; Delerue, C.; Allan, G.; Hens, Z. *ACS Nano* **2009**, *3*, 3023.
(19) Moreels, I.; Lambert, K; Muynck, D. D.; Vanhaecke, F.; Poelman, D.; Martins, J. C.; Allan, G.; Hens, Z. *Chem. Mater.* **2007**, *19*, 6101.
(20) Sheik-Bahae, M.; Said, A. A.; Wei, T. H.; Hagan, D. J.; Van Stryland, E. W. *IEEE J. Quantum Electron.* **1990**, *26*, 760.
(21) Xu, C.; Webb, W. W. *J. Opt. Soc. Am. B* **1996**, *13*, 481.

DOI: 10.1021/nl1018673 | *Nano Lett.* **2010,** *10,* 3577--3582